Noise Reduction Technologies for Wind Turbines

Michaela Herr, Roland Ewert, Benjamin Faßmann, Christof Rautmann, Susanne Martens, Claas-Hinrik Rohardt and Alexandre Suryadi

Abstract Results from a numerical and experimental aeroacoustic assessment of 2D wind turbine blade sections are presented. CFD/CAA-based predictions using a synthetic turbulence method were conducted at a NACA 64-618 profile as well as at a new low-noise airfoil design RoH-W-18%c37. Validation experiments were performed in DLR's Acoustic Wind-Tunnel Braunschweig (AWB) for varying transition locations. A trailing-edge noise reduction benefit of 2–4 dB in overall sound pressure level was predicted for the new airfoil under design conditions. A large laminar extent of the boundary layer significantly reduces the noise emission (by up to 8 dB) compared to equivalent cases with forced transition at the leading edge. An additional noise reduction (with realistic reductions of the peak levels by 4–6 dB) was accomplished by flow-permeable trailing-edge extensions which were successfully transferred to the two profiles from forerunner aerospace-related studies.

1 Introduction

According to current knowledge trailing-edge noise (TEN) as generated in the outer 20–25% of the rotor radius represents the most relevant noise contributor at modern large wind turbines. Important indicators to support this statement are i) measurements of noise radiation directivities corresponding to the typical TEN cardioid-type

Michaela Herr, Benjamin Faßmann, Claas-Hinrik Rohardt and Alexandre Suryadi
German Aerospace Center (DLR), Institute of Aerodynamics and Flow Technology, Lilienthalplatz 7, D-38108 Braunschweig, Germany; e-mail: michaela.herr@dlr.de

Christof Rautmann
Nordex Energy GmbH, Blade Engineering, Aerodynamics & Structural Mechanics, Langenhorner Chaussee 600, D-22419 Hamburg, Germany

Susanne Martens
Leibnitz Universität Hannover, Institute of Turbomachinery and Fluid Dynamics (TFD), Appelstraße 9, D-30167 Hannover, Germany

characteristics, ii) noise source localization results at wind turbine rotor blades acquired with phased microphone arrays, and finally, iii) the experimentally proven efficiency of trailing-edge modifications on overall wind turbine noise in field measurements [12, 13, 14]. TEN at rotor blades is generally modeled as 2D problem while separating the rotor in distinct blade elements. Its key mechanism is the fluctuating pressure induced by the boundary-layer turbulent eddies and its propagation to the farfield due to the scattering from the trailing edge (TE) [4, 9]. The overall blade noise is then estimated through summation of the respective radial contributions that are calculated based on the local and overall operational conditions. Typically, the contribution of blade tip noise, attributable to 3D tip vortex formation, is negligible. An acoustically driven blade design conventionally foresees a reduced loading, i. e. reduced power production in the very tip region. Since published field test data are still limited, the relevant literature does not provide clear statements concerning the importance of additional flow-induced noise sources, i. e. flow separation noise (which is intended to be strictly avoided by the blade design and pitch control, but could eventuate during operation) and turbulent-inflow leading-edge interaction noise. The noise ranking of the latter two contributions appears individually dependent on the turbine type and site quality.

1.1 Scope of Research

The wind energy project BELARWEA[1] aims at the development and validation of improved methods to support the design of both efficient and low-noise wind turbine rotors. Aeroacoustically driven 2D profile design, 3D winglet design and 2D/3D CFD and CAA analysis are supplemented by the transfer of passive noise reduction add-on technologies from aerospace applications to wind turbine blades. Based on a down-scaled version of the open source NREL-5-MW reference rotor [10], a noise reduction of at least 3 dB at a given rotor performance is targeted by a dedicated 3D redesign of the outer 20% of the rotor radius. Experimental demonstration and tool validation shall be provided in systematic validation steps, i .e.

- at 2D blade sections in the Acoustic Wind-Tunnel Braunschweig (AWB) of DLR, and
- at 3D blade tips in the larger acoustic facility DNW-NWB[2], operated by the German-Dutch Wind-Tunnels foundation.

The following documentation summarizes the first set of 2D aeroacoustic simulations and AWB measurements, yielding a detailed matrix of the relevant system parameters aerodynamic performance vs. noise. The focus is set on the acoustic evaluation of two different profile geometries, the NACA 64-618 profile as installed

[1] The German acronym BELARWEA (”Blattspitzen für Effiziente und LärmArme Rotoren von WindEnergieAnlagen”) stands for ”blade tips for efficient and low-noise wind turbine rotors”.

[2] DNW: German-Dutch Wind-Tunnels (Deutsch-Niederländische Windkanäle); NWB: Low-Speed Wind-Tunnel Braunschweig (Niedergeschwindigkeits-Windkanal Braunschweig).

in the outer 29–33%[3] of the 5-MW NREL reference rotor radius [10], and a new profile design RoH-W-18%c37 developed in BELARWEA. For confidentiality reasons the corresponding geometry and pressure distribution data of the latter are disclosed from this report.

2 Approach

The herein documented 2D analysis contains the following three subsequent steps:

1. numerical (CFD and CAA) simulations for design conditions to estimate the aeroacoustic benefits under assumed typical operational conditions;
2. equivalent numerical simulations, but for (smaller scale, lower velocity) test conditions present during the AWB measurements;
3. wind-tunnel testing in the AWB
   - to provide validation data for varying free stream velocities u_∞, angles of attack α and turbulent boundary-layer (TBL) transition locations, and
   - to rank order the TEN reduction capabilities related to i) the partially laminar extent of the TBL, interrelated with ii) the profile geometry, and to iii) aerodynamically acceptable TE add-ons with the potential to modify the scattering of pressure fluctuations into sound.

The design conditions in BELARWEA represent a deliberate compromise between the conditions at the 5-MW NREL rotor and typical wind-tunnel conditions[4] because the project aims first of all at the validation of the applied design and analysis processes prior to their application to a specific product development. These scaled operational conditions / design conditions were:

- Reynolds number $Re = 3$ Mio. ($u_\infty = 68$ m/s),
- Mach number $M = 0.2$,
- chord length $l_c = 0.65$ m,
- targeted lift coefficient $c_L = 1.15$.

Test conditions in the AWB were:

- $Re = 0.82$–1.28 Mio. ($u_\infty = 40$–60 m/s),
- $M = 0.118$–0.176,
- $l_c = 0.3$ m,
- targeted $c_L = 1.15$.

[3] An exact number cannot be provided here because the NREL 5-MW model rotor is defined in terms of blade elements, i. e. areas of intermediate profiles are not explicitly indicated.

[4] Note that the (offshore) NREL 5-MW model rotor is not representative for typical onshore wind turbines. In a classical 2D experiment these selected conditions are realizable in DNW-NWB.

2.1 Numerical Approach

The numerical approach pursued in BELARWEA relies on a hybrid two-step procedure for a first-principle based prediction of broadband TEN. The first step rests on a CFD RANS simulation (here: applying the DLR TAU code with Menter SST turbulence model) of the time-averaged turbulent flow around the airfoil. In the second step, a CAA simulation (applying the DLR PIANO code) is carried out solving time-dependent linear equations on structured multi-block meshes. For the preparation of unsteady vortex sound sources a synthetic turbulence method (Fast Random Particle Mesh method, FRPM [2, 3]) is used to force the linearized applied acoustic perturbation equations. FRPM realizes a '4D' time-space based prediction of fluctuating sources in a restricted volume around the TE region, including the convection of synthetic eddies with proper imposed time decay.

The TEN prediction capabilities and associated ongoing further-development of PIANO-FRPM have been continuously documented within an ongoing series of workshops devoted to Benchmark Problems for Airframe Noise Computations (BANC) [1, 6, 7]. For detailed cross-comparisons with results from alternative prediction and measurement approaches at a first set of airfoils (NACA 0012, DU 96-W180, NACA 64-618 at higher Re) the interested reader may refer to the BANC documentation and the related further reading referenced therein. For a comprehensive documentation of the newly established semi-automatized TEN prediction process chain and 'best practice' recommendations applied in BELARWEA cf. [15].

2.2 Experimental Approach

TEN measurements were performed in DLR's AWB which is a free-jet, low-noise facility with an open test section. Farfield TEN was measured using a directional microphone system with an elliptical reflector (i. e. two foci, I = source and II = microphone) pointing towards the pressure side of the model (Fig. 1 left). The system, data processing and necessary corrections to derive absolute farfield TEN levels are documented in [5]. For direct comparisons all shown acoustic (numerical and experimental) data are referenced to a 1-m span and a 1-m observer distance from the convection-corrected TE source location, referring to a 90° observation angle to the wind-tunnel center line. TEN spectra are presented in 1/3-octave bands.

The challenges and limitations of airframe noise benchmark measurements have been recently reviewed in [1]. One severe limitation lies in the frequency-dependent resolution of focusing measurement systems (i. e. their low resolution at low frequencies) that are required for TEN measurements due to generally very low signal-to noise ratios. In open-jet wind-tunnels like the AWB, excess noise as generated at the model/side-wall junctions typically sets the low-frequency limit of the usable measurement range of TEN. From cross-comparisons among available TEN benchmark data [1, 7] it is known that today's TEN databases do not provide meaningful data significantly below 1 kHz, i. e. in a frequency range that encompasses the TEN

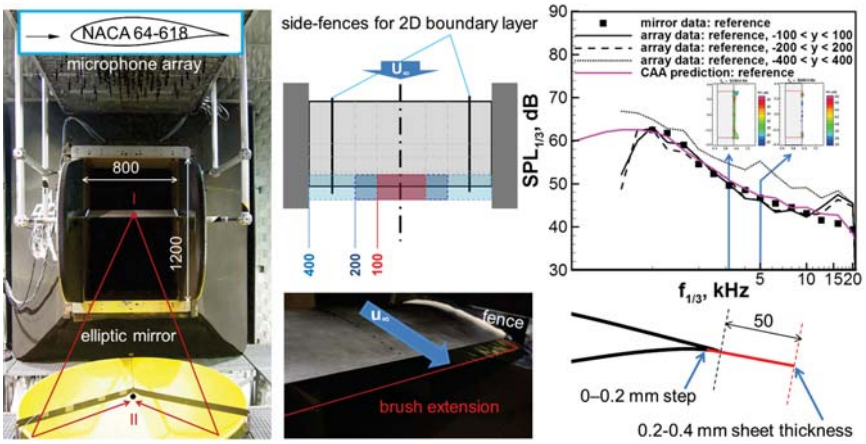

Fig. 1 Test setup in the AWB (dimensions in mm). Top center: View from top; definition of integration areas (red and blue colors) selected for the additional microphone array data post processing. Top right: Example validation data set with comparison of microphone array (source maps and spectra derived with the CLEAN-SC algorithm for varying spanwise extent of the integration area) vs. elliptic mirror microphone data. Bottom center and right: installation of low-noise TE add-ons.

spectral peaks in many of the technologically relevant cases. In the present study data were contaminated at $f_{1/3} < 1$ kHz, and $f_{1/3} < 1.25$ kHz for test cases with significant TEN reductions. The respective frequency bands were, therefore, excluded from the analysis. Due to its system-inherent high gain, the AWB mirror system generally outperforms equivalent phased array setups in the higher frequency range. That is why the mirror setup is preferably used in particular for the evaluation of low-noise configurations. In the current setup, where a microphone array arrangement was additionally mounted above the model for cross-checks on the detrimental corner sources, results from the mirror are reproducible by the array only for limited test cases with sufficient signal-to-noise ratios, i. e. when the respective array source maps clearly indicate the presence of a line source at the TE (Fig. 1 top right).

3 Results

The following analysis was made for the two bracketing cases of i) a TBL with natural transition, corresponding to an hydraulically smooth 'clean' profile surface as well as of ii) a fully turbulent boundary-layer, corresponding to a 'dirty' profile surface. In the first set of numerical simulations, summarized in section 3.1, the denomination 'NAT' defines natural transition for negligible $< 0.1\%$ inflow turbulence level, whereas 'FUL' stands for a fully turbulent boundary layer right from the leading edge. In section 3.2, where simulations are directly compared with respective AWB measurement results, the fully turbulent case was approximated by tripping of the boundary layer at 5% on the suction side and at 10% on the pressure side. Due

to the low *Re* numbers in the AWB, non-tripped boundary layers on the new RoH-W-18%c37 profile develop laminar separation bubbles on both sides of the airfoil; to provide a more realistic comparison with the high-performance 'NAT' cases under design conditions the boundary layers were tripped at 42% on the suction side and at 57% on the pressure side. For the NACA 64-618 the boundary layers could remain untripped in the 'clean' cases, and corresponding simulations were performed accounting for an inflow turbulence level of 0.3–0.4% in the AWB.

3.1 Simulation Results for Design Conditions vs. AWB Conditions

Fig. 2 provides a first overview on the predicted effects of *Re* number, $c_L(\alpha)$ and TBL extent ('FUL' vs. 'NAT') on TEN. Both aerodynamic (top figures) and acoustic polars (bottom figures) are presented for AWB vs. design conditions, as specified in section 2. Overall sound pressure levels (OASPL, non weighted and A-weighted to approximate subjective human perception) are derived from integration of the TEN

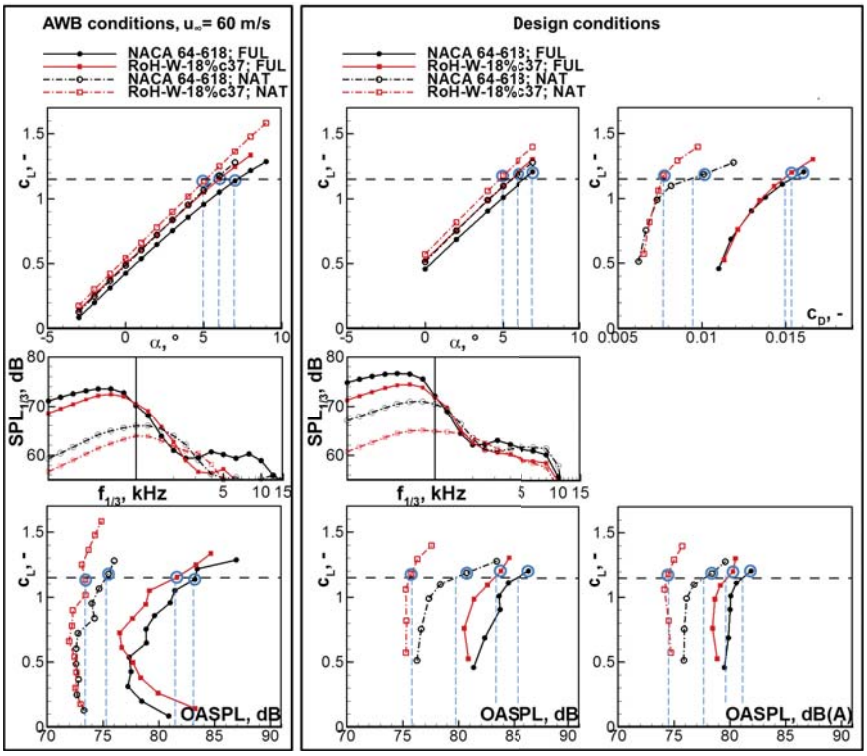

Fig. 2 Simulation results for AWB (left) vs. design conditions (right). For details cf. the text. A-weighted TEN as well as classical lift-over-drag polars $c_L(c_D)$ (figures on the right) are rather of interest for design/'operational' conditions and are not shown for the lower *Re* AWB experiment.

1/3-octave bands with center frequencies of 125 Hz $\leq f_{1/3} \leq$ 12.5 kHz. In addition to that, 1/3-octave band spectra $\mathrm{SPL}_{1/3}(f_{1/3})$ are shown (center figures) for the four simulation conditions (two profiles at 'FUL' or 'NAT', respectively) which were closest to the target c_L (marked by the dashed horizontal line in the figures). From this survey the following conclusions can be made:

- TEN OASPL can be significantly reduced (here, by up to 8 dB / 6 dB(A) for design conditions) when extended laminar boundary layer regions can be realized.
- Profile shape, i. e. a redefinition of the static pressure distribution, can lead to an additional noise benefit; in the current study a 3–4 dB / 2–3 dB(A) reduction in OASPL is predicted for design conditions, as mainly accomplished through reductions in the low-frequency TEN peak region (1-kHz limit of the AWB measurement marked by the black vertical lines in the figures).
- Reduction of the model scale, i. e. reduction of *Re* diminishes the noise benefit of the RoH-W-18%c37 when compared to design conditions.

3.2 Validation with AWB Measurement Data

Fig. 3 surveys farfield 1/3-octave band TEN spectra for three distinct geometric angles-of-attack α_g in the AWB. The corresponding aerodynamic angles-of-attack α set in the simulations, i. e. the necessary corrections for the free-jet flow deflections, were determined through cross-comparisons of the simulated (target) and measured static pressure distributions. One important drawback of the current

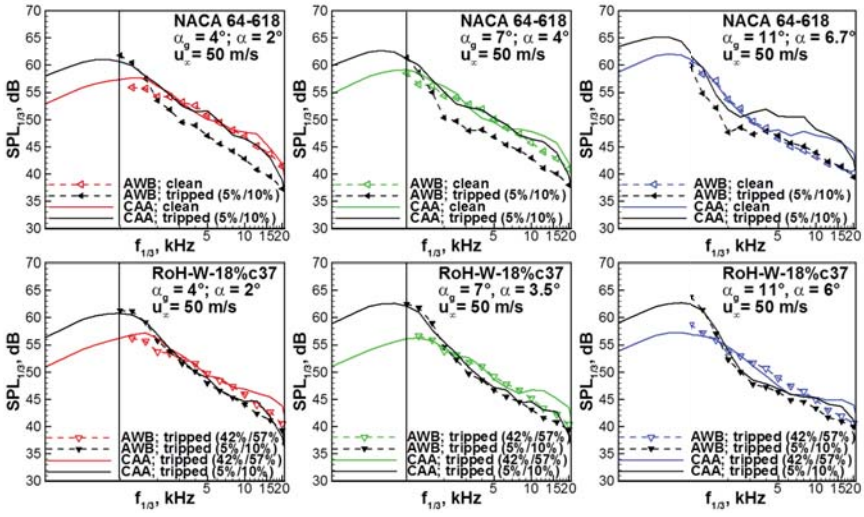

Fig. 3 Comparison of CAA predictions with AWB directional microphone measurement data; effect of TBL transition position. The vertical lines mark the 1-kHz 1/3-octave band center frequency.

dataset lies in the fact that design conditions could not be well-reproduced for the tripped NACA 64-618 in the AWB experiment. As deducible from Fig. 4 (bottom), the target $c_L = 1.15$ can only be achieved for a corresponding α_g with massive TE separation. Given the aforementioned low-frequency limitation of the measurement, the expected noise reduction benefits of the RoH-W-18%c37 are only visible when comparing the corresponding 'clean' cases (Fig. 4 top left). Note that the intersection of the two spectra, indicating noise reduction or noise increase compared to the NACA 64-618, is well captured. According to Fig. 3, the predictions for the RoH-W-18%c37 profile are almost perfectly confirmed by the measurements. The inherent significant noise reduction potential of laminar airfoil designs, providing large laminar boundary-layer portions is pinpointed. However, prediction fails for all tripped NACA 64-618 cases which can be only partly explained by the presence of TE separation in the experiments. A more detailed aerodynamic assessment is required for clarification of the observable discrepancies at $\alpha_g < 11°$. Predictions for the 'clean' NACA 64-618 are in the contrary well represented by the measurement.

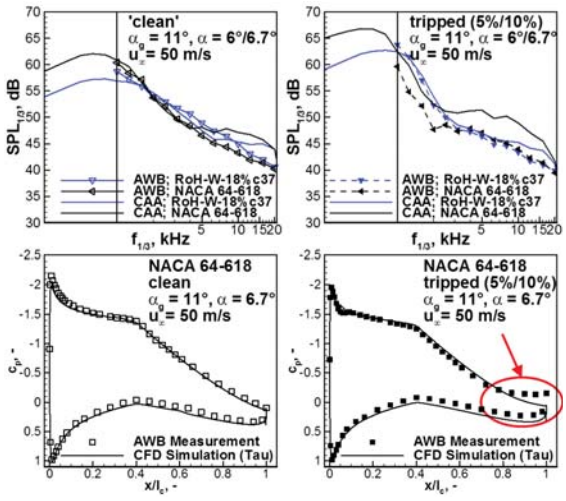

Fig. 4 Comparison of CAA predictions with AWB directional microphone measurement data; (top) TEN levels at conditions closest to the design target (NACA 64-618 vs. RoH-W-18%c37) and corresponding static pressure distributions for the NACA 64-618.

3.3 Additional Noise Reduction Potential through TE Extensions

A rough indicator for the additional noise reduction potential through flow-permeable TE add-ons is given in Fig. 5. Due to space limitations only selected results are shown with reference to the new low-noise design RoH-W-18%c37. Note that these add-ons were realized as TE extensions according to Fig. 1 (bottom center and right); dependent on the respective configurations, lift remained unchanged or was increased compared to the unmodified airfoil. The rationale behind the selected add-

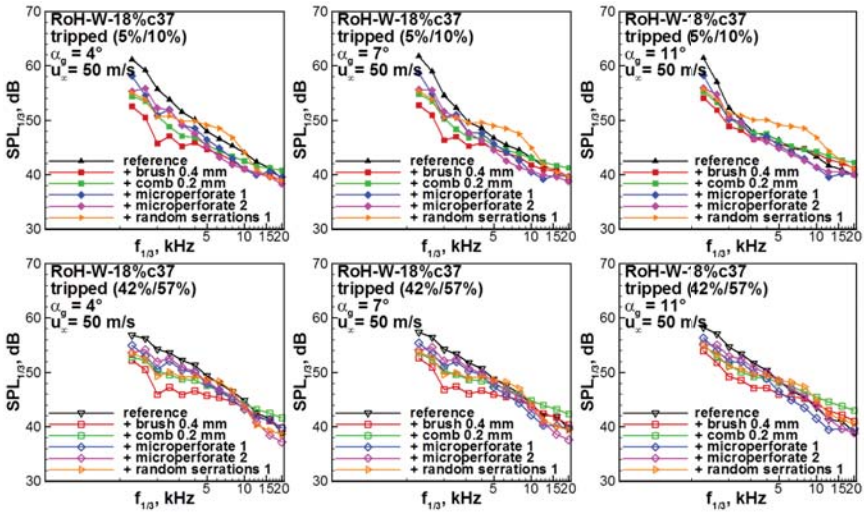

Fig. 5 Effect of selected TE extensions on TEN spectra for the RoH-W-18%c37 with varying transition locations.

ons as well as design recommendations and underlying scaling laws were reported in earlier work [5, 8]. The new contribution documented here consists in the successful adaptation of the above concepts (porous, slotted or brush-type extensions) to the new airfoil geometries, dedicated to wind energy applications. Compared to (stiff) TE serrations that are currently used as standard noise reduction technologies at todays' wind turbine rotors [11, 12], the proposed concepts appear less susceptible to excess noise generation.

4 Conclusions

This communication summarizes the results from a 2D aeroacoustic study, dedicated to the design of low-noise airfoils for wind energy rotors. CFD/CAA based predictions with stochastic source reconstruction were successfully applied to predict the trailing-edge noise of a new airfoil (RoH-W-18%c37) for varying turbulent boundary-layer transition locations. Both numerical and experimental results indicate that the overall performance of a purely laminar airfoil design will be significantly limited if inflow turbulence levels, blade wear-out or manufacturing accuracy cannot guarantee idealized conditions with maximum laminar boundary layer extents during operation. In the current study, an up to 8 dB noise increase was observed for the corresponding fully turbulent cases. The noise emission of an aeroacoustically driven design can be further significantly reduced by well-adjusted flow-permeable edge-extensions. Open questions refer to discrepancies when comparing

simulation and measurement results for the tripped NACA 64-618 reference profile in the current study. Moreover, due to measurement limitations in the low-frequency range, a comprehensive final assessment of the RoH-W-18%c37 should also involve surface pressure measurements in the trailing-edge region to finally confirm the predicted noise reduction at low frequencies through nearfield measurements.

Acknowledgements This work has been conducted within the project BELARWEA (ref. 0325726) funded by the German Federal Ministry for Economic Affairs and Energy (BMWi).

References

1. M. Choudhari, C. Bahr, M. Khorrami, D. Lockard, L. Lopes, N. Zawodny, M. Herr, Pott-Pollenske, M. M., Kamruzzaman, T. van de Ven, E. Manoha, S. Redonnet, K. Yamamoto, T. Ikeda, and T. Imamura. Simulations & Measurements of Airframe Noise: A BANC Workshops Perspective. Proceedings of NATO STO-MP-AVT-246 Specialists Meeting on Progress and Challenges in Validation Testing for Computational Fluid Dynamics, Avila, Spain, September 26–28, 2016.
2. R. Ewert. Broadband Slat Noise Prediction Based on CAA and Stochastic Sound Sources from a Fast Random Particle-Mesh (RPM) Method. *Computers & Fluids*, 37:369–387, 2008.
3. R. Ewert, J. Dierke, J. Siebert, A. Neifeld, C. Appel, M. Siefert, and O. Kornow. CAA Broadband Noise Prediction for Aeroacoustic Design. *Journal of Sound and Vibration*, 330(17):4139–4160, August 2011.
4. J. E. Ffowcs Williams and L. H. Hall. Aerodynamic Sound Generation by Turbulent Flow in the Vicinity of a Scattering Half Plane. *Journal of Fluid Mechanics*, 40(4):657–670, 1970.
5. M. Herr. *Trailing-Edge Noise—Reduction Concepts and Scaling Laws*. Dissertation, Technical University Braunschweig, Germany, DLR report 2013-32, ISSN 1434-8454, ISRN DLR-FB-2013-32, September 2013.
6. M. Herr, R. Ewert, C. Rautmann, M. Kamruzzaman, D. Bekiropoulos, A. Iob, R. Arina, P. Batten, S. Chakravarthy, and F. Bertagnolio. Broadband Trailing-Edge Noise Predictions—Overview of BANC-III Results. AIAA Paper AIAA 2015-2847, June 2015.
7. M. Herr and M. Kamruzzaman. Benchmarking of Trailing-Edge Noise Computations—Outcome of the BANC-II Workshop. AIAA Paper AIAA 2013-2123, May 2013.
8. M. Herr, K.-S. Rossignol, J. Delfs, M. Mößner, and N. Lippitz. Specification of Porous Materials for Low-Noise Trailing-Edge Applications. AIAA Paper AIAA 2014-3041, June 2014.
9. M. S. Howe. A Review of the Theory of Trailing Edge Noise. *Journal of Sound and Vibration*, 61(3):437–465, 1978.
10. J. Jonkman, S. Butterfield, and W. Musial und G. Scott. Definition of a 5-MW Reference Wind Turbine for Offshore System Development. NREL Technical Report NREL/TP-500-38060, Februar 2009.
11. S. Oerlemans. Research and Development of Low-Noise Blade Add-on Devices. Presentation at the workshop "Serration Technology on Airfoil: Unsteady Aerodynamic and Aeroacoustics", Leiden, The Netherlands, October 17–21, 2016.
12. S. Oerlemans. Reduction of Wind Turbine Noise using Blade Trailing Edge Devices. AIAA Paper 2016-3018, June 2016.
13. S. Oerlemans, M. Fisher, T. Maeder, and K. Kögler. Reduction of Wind Turbine Noise using Optimized Airfoils and Trailing-Edge Serrations. *AIAA Journal*, 47(6):1470–1481, 2009.
14. S. Oerlemans, P. Sijtsma, and B. Méndez López. Location and Quantification of Noise on a Wind Turbine. *Journal of Sound and Vibration*, 299:869–883, October 2007.
15. C. Rautmann. *Numerical Simulation of Wind Turbine Trailing-Edge Noise*. Dissertation, Technical University Braunschweig, Germany, 2017 (not yet published).